Response to reviewers' comments

on the paper "Influence of simple terrain on the spatial variability of a low-level jet and wind farm performance in the AWAKEN field campaign"

submitted to Wind Energy Science

Submission due on April 4 2025

Regular font – Reviewers
Bold – Our response to reviewers

RC1: 'Comment on wes-2024-166', Anonymous Referee #1, 19 Jan 2025

#GC1 In this article, the authors investigated the impact of 'simple terrain' (characterized by slight elevation variations of less than 50 m) on wind farm power production under stable stratification with Low-Level jets (LLJs). The study utilized WRF-LES-GAD simulations and corroborated with the observational data from wind farms at the AWAKEN site. The article is well-written and the addressed details on the impact of simple terrain on wind farm performance is beneficial to wind energy community. I recommend for the publication of this article by addressing my minor comments on technical details as follows.

We appreciate the positive feedback from the reviewer and will do our best to address the recommendations.

#GC2 It is unclear how the frictional velocity was evaluated for the chosen site based on the requirements outlined in lines 134–136 to determine the necessary grid resolution.

Even though the requirement was a friction velocity lower than 0.5 m/s, the heat flux being smaller than -20 W/m^2 (~ −57 W/m^2) suggests strong turbulence for nighttime. We imposed the upper limit to the friction velocity because, above that threshold, the hub height winds speeds tend to be much larger than 10 m/s, and the turbines in the first row operate near, at, or above rated capacity. That would make it difficult to evaluate the spatial variability in performance and the wakes. With that in mind, we selected the case with the highest friction velocity (~0.35–0.40 m/s, a relatively high value for nighttime hub height wind speeds of about 8 m/s during the nighttime) among the three nights that passed all the filters. This date combines relatively strong turbulence with not-too-strong hub height wind speeds, which is excellent from the point of view of our targeted research scope. Regarding the spatial resolution being sufficient for this level of turbulence, Sanchez Gomez et al. (2022) (see their Appendix) carried out a grid sensitivity study at the same site with WRF-LES-GAD for a weaker LLJ (maximum nose speed of about 21 m/s, in comparison with 25 m/s in our study) and found that a horizontal grid resolution of about 4 m was sufficient to resolve most of the turbulence above 30 m AGL. Comparing the turbulence levels in their case to ours, the observed hub height vertical velocity variance was above 0.15 m/s in their study, whereas it was 0.21 m/s in ours (about 33% larger). Thus, we conclude we can resolve most of the turbulence with a 5 m resolution grid, as further demonstrated by our agreement with observations.

We incorporated a more detailed explanation for our grid resolution choice and a citation to Sanchez Gomez et al. (2022) in lines 159-165, as below:

“The innermost nest domain (D3) has a fixed horizontal resolution of $\Delta x=$~5~m, determined based on a grid sensitivity study conducted at the same site using WRF-LES-GAD for a weaker LLJ case (see the Appendix of Sanchez Gomez et al. (2022)). Their study shows that most turbulence above 30 m AGL is adequately resolved

with a 3.94 m grid. In our LLJ case, turbulence is stronger, with a vertical velocity variance of approximately 0.21 m²/s² at 90 m AGL, compared to 0.15 m²/s² in their study. To ensure turbulence is adequately resolved, we use a 5 m grid in the innermost domain.”

#GC3 Details regarding the simulation setup for domains D1, D2, and D3 are not sufficiently clear, particularly how the simulations were conducted. Including a flowchart of the simulation setup, either in the Appendix or Section 2.2, would help clarify this. Such a flowchart could detail the initial conditions based on the HRRR model and their integration with the GAD framework, which would be beneficial for readers.

We have included a flowchart of the simulation framework that is focused on the communication between the input data (HRRR) and the WRF domains via initial and lateral boundary conditions (I/LBCs) in Appendix D. It also briefly describes how the CPM and the GAD integrate the multiscale framework.

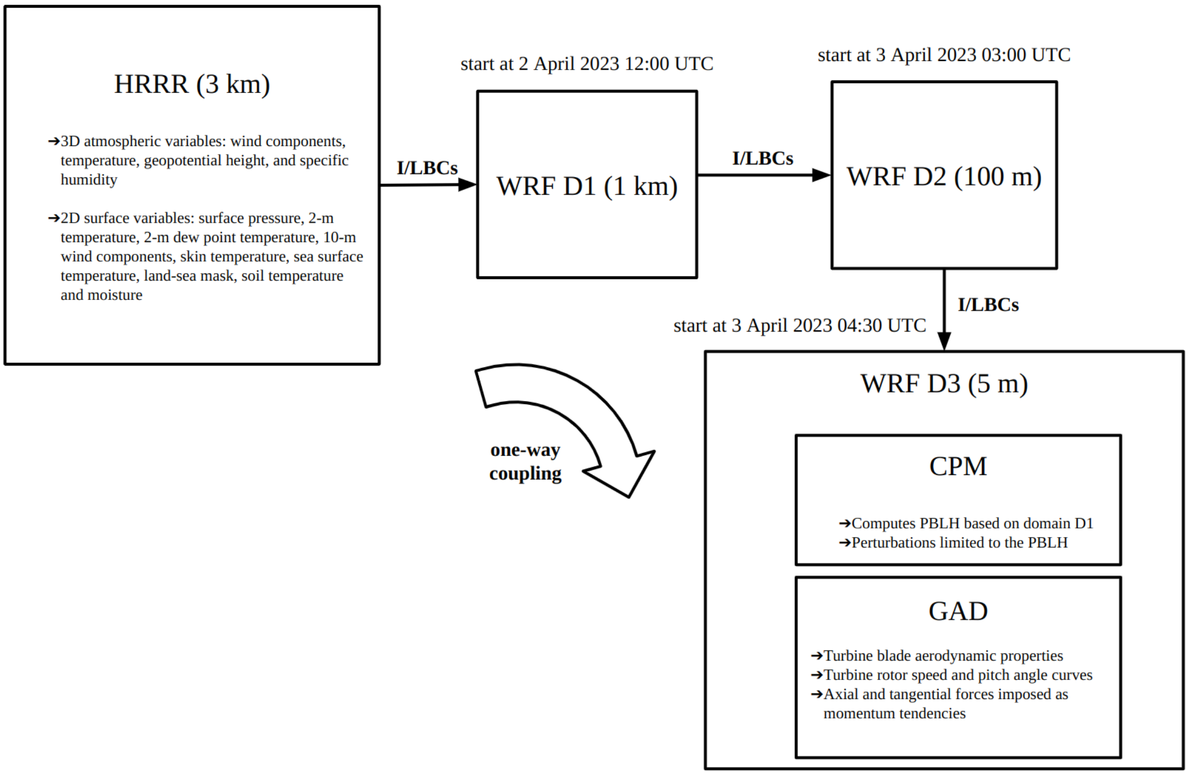

Figure D1 – Multiscale simulation flowchart: The HRRR analysis dataset (hourly frequency) provides initial and lateral boundary conditions (I/LBCs) for the mesoscale domain D1 in WRF. The nested LES domains D2 and D3 receive I/LBCs from their respective parent domains (D1 and D2) through one-way coupling, meaning no feedback occurs to the parent domains. To reduce computational cost, the domains are activated sequentially in time. The Cell Perturbation Method (CPM) and Generalized Actuator Disk (GAD) are applied only in the innermost domain D3.

#GC4 What do the black vertical lines in Figures 11 and 12 represent? Additionally, what is the significance of the dotted lines in Figure 4? I would expect them to indicate the tips of the wind turbine blades; however, please confirm this and make any necessary changes to the figure captions.

The black vertical lines in Figures 11 and 12 are the projected positions of the H05, G02, and F04 turbine rotors onto the vertical plane. Also, the reviewer is correct about Figure 4. The dotted horizontal lines represent the rotor top and bottom tips of the turbines. Finally, we have adjusted the captions of Figures 4, 11 and 12, as below:

Figure 4. Vertical profiles of wind speed (a), direction (b), potential temperature (c), TI (d) and $w'w'$ (e) for a 30 minute window between 04:55 and 05:25 UTC. Observations from the scanning lidar at site A1 (OBS-A1-SL), the profiling lidar at site A1 (OBS-A1-PL), and the AERI at site C1 (OBS-C1-AERI) are represented as markers. Results from domain D3 are represented as blue continuous lines. The dotted horizontal lines represent the rotor top and bottom tips of the turbines.

Figure 11 – Figure 11. Vertical cross-section of wind speed difference relative to the front row profile ($WS - WS_{fr}$) for domain D3 in the simulation without turbines. The LLJ nose height is also displayed (a). Wind speed difference along terrain-following lines at fixed heights AGL (b). The black vertical lines indicate the projected positions of turbine rotors H05, G02, and F04 onto the vertical plane.

Figure 12 – Vertical cross-section of wind speed difference relative to the front row profile ($W S - W S_{fr}$) for domain D3 in the simulation without turbines, with streamlines of the mean flow located between 20 and 600 m AGL near the inlet (a). The remaining subplots show the vertical displacement along the streamlines (Δz, b), actual change in wind speed along the streamlines (ΔWS_{str}, c), estimated change in wind speed caused by the vertical displacement of the LLJ (ΔWS_{vert}, d) and the estimated total change in wind speed of (c) and (d) combined (ΔWS_{tot}, e). The aforementioned variables are relative to the value at the front row The black vertical lines indicate the projected positions of turbine rotors H05, G02, and F04 onto the vertical plane.

#GC5 The variables used in the text are typeset with LaTeX, whereas those in the figures are not. While this is a minor point, maintaining consistency between the text and figures would enhance the overall presentation.

We appreciate the reviewer's attention to detail, and we agree that having the Figures with variables consistently typeset improves the manuscript. Thus, we have modified all the Figures with the same rule such as shown in Figure 3.

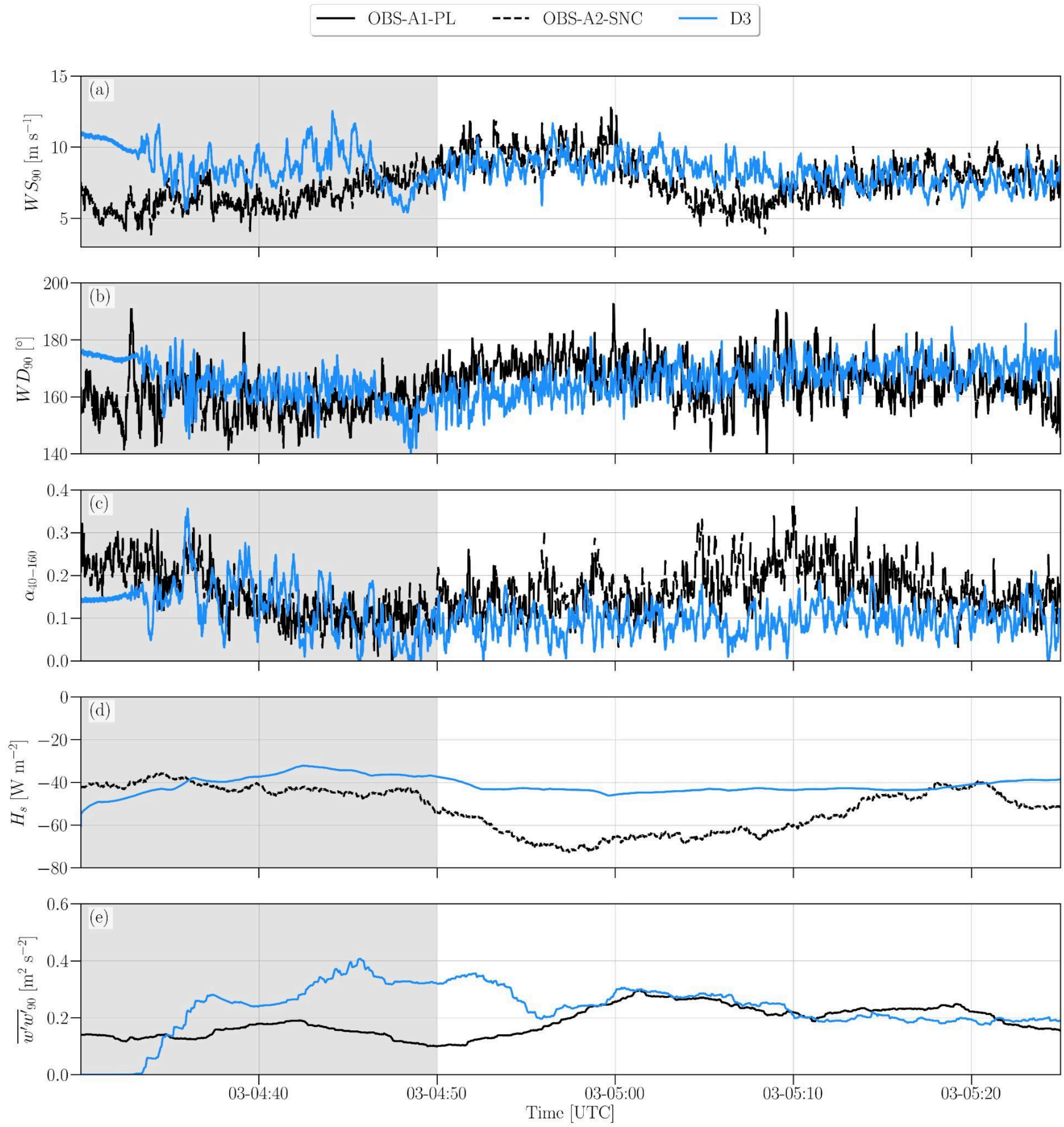

Figure 3 – Example of variables now typeset with LaTeX.

References

Sanchez Gomez, M., Lundquist, J. K., Mirocha, J. D., Arthur, R. S., Muñoz-Esparza, D., & Robey, R. (2022). Can lidars assess wind plant blockage in simple terrain? A WRF-LES study. *Journal of Renewable and Sustainable Energy*, *14*(6), 063303. https://doi.org/10.1063/5.0103668

RC2: 'Comment on wes-2024-166', Anonymous Referee #2, 07 Mar 2025

This paper focuses on a strong low-level jet (LLJ) event under stable conditions during the AWAKEN campaign, investigating how simple terrain modulates flow and wake fields. Specifically, it examines how terrain-induced effects contribute to spatial variability in the flow field. For the simulation, the authors employ a multiscale modeling framework (WRF-LES-GAD) alongside available SCADA data. The study presents interesting findings with a valuable contribution to the field. Publication is recommended after addressing the comments provided for further clarity and accuracy.

General comments

#GC1 I appreciate the authors' effort in integrating several interesting concepts into the manuscript. Given the space constraints, some of my comments stem from the manuscript's structure and the concepts addressed. For instance, while the study provides insights into the specific LLJ event analyzed, it does not sufficiently elaborate on its generation mechanism.

We recognize the value of understanding and contextualizing the generation mechanism of the LLJ to this study, despite that not being the focus of the paper. The genesis and evolution of the nocturnal LLJ occur over several hours, and our study looks at essentially a "snapshot" of that process. The generation mechanism for the LLJ in the SGP has been associated with the combination of frictional decoupling, sloping terrain, and synoptic PGF. As shown by Smith et al. (2019), the LLJ exhibits substantial heterogeneity in depth, wind speed, and direction, which can influence regional convergence patterns and even contribute to thunderstorm formation over the sloping west-east terrain.

A key connection to our study is that terrain-induced effects further modify an already heterogeneous process. When assessing wind farm performance on a broader scale, both the large-scale spatiotemporal variability described by Smith et al. (2019) and localized terrain effects should be considered. Additionally, the LLJ's temporal evolution typically involves wind intensification, boundary layer deepening, and clockwise wind rotation, all of which interact with terrain features to shape the spatial variability in wind speed.

Thus, we have improved the relevance of the generation mechanism and evolution of the LLJ in the paper to the problem of the spatial variability in wind speed and farm performance. We modified this sentence in the Introduction:

“The physical mechanisms that form LLJs generally involve nocturnal frictional decoupling, sloping terrain, and synoptic pressure gradient forces..”

To clarify the aforementioned connections, we have also added the following sentences to the manuscript at the end of Section 4.1:

“The temporal evolution of the LLJ typically involves wind intensification, deepening of the stable boundary layer, and clockwise rotation, a process that is inherently heterogeneous across the SGP (Smith et al., 2019). Local terrain-induced effects further amplify this variability. When assessing wind farm performance at larger scales, both the broader spatiotemporal variability described by Smith et al. (2019) and localized terrain influences must be considered.”

#GC2 The paper presents several interesting findings and interpretations, particularly regarding the cross-sectional plot of KHI in Fig. 7, which effectively illustrates the flow field. However, I was expecting further discussion or analysis on how the observed instability may or may not influence the flow field or more specifically wind streamlines both above and within the wind park. Given that such instabilities can locally impact turbulence, wake dynamics, and momentum transfer, it would be important to explore whether KHI explicitly or implicitly plays a role in shaping the flow field. Including this discussion could strengthen the interpretation of the results and enhance their relevance to wind farm performance.

We thank the reviewer for their interest in this process. While KHIs are not the central focus of our study, their influence on the flow field can be categorized into two key effects: (i) enhanced turbulent mixing, which tends to be intermittent in time (Blumen et al., 2001; Newsom and Banta, 2003; Malekmohammadi et al., 2025) and spatially heterogeneous (Coulter & Doran, 2002; Zhou and Chow, 2014); and (ii) modifications to the mean wind and stratification profiles resulting from the mixing events in (i).

As such, KHIs can influence the spatial variability in wind speed by enhancing vertical momentum transport and weakening thermal stratification. Specifically, the enhanced mixing (i) can transport momentum downward from the LLJ core, accelerating wake recovery, while the altered mean state (ii) can increase near-surface wind speeds and reduce stratification. These changes act to reduce the terrain-induced spatial heterogeneity in wind speeds, as discussed in Section 4.1.

For example, it is plausible that, had KHIs not been triggered in the simulation, the spatial variability in wind speed would have been greater. While this remains a logical inference rather than a demonstrable result with the available evidence, it aligns with the mechanisms outlined in the literature and complements our current findings.

A more detailed investigation into the role of KHIs would require domains that are both (a) sufficiently resolved to capture the small-scale structures of KHIs and (b) large enough to account for their spatial heterogeneity. The stable boundary layer (SBL) characteristics—such as wind speed, direction, thermal stratification, shear, and veer—vary across the domain due to terrain and surface roughness, which leads to spatial and temporal intermittency of KHI formation (Coulter & Doran, 2002).

As for the influence of the KHI on the streamlines of the time-averaged flow field, that is harder to tell because several processes simultaneously influence such streamlines. An investigation with idealized LES simulations of an LLJ flow over terrain with and without KHI would be able to isolate this process, and thus be better equipped to address this point. We note, however, that the inverse problem is also interesting, that is, "how the mean flowfield influences/generates the KHIs". As we discussed in the subsequent point raised by the reviewer, the commonly reported mechanism for KHI generation is enhanced wind shear in stable boundary layers (SBLs) (Newsom and Banta, 2003; Blumen et al., 2001). For instance, Newsom and Banta (2003) describe how low-level wind deceleration enhances wind shear, leading to KHIs. In the present investigation, a plausible argument is that the terrain-induced low-level deceleration upstream of King Plains (Figs. 8b and 10b) increases the wind shear and triggers the KHI. Thus, the problem of how the KHI influences the flow field and vice versa is a rich topic and excellent motivation for future studies.

In a new paragraph that furthers the discussions on the KHI, we have included more references and connected them to our work, lines 315–318:

"A plausible explanation for the observed KHI formation in our investigation is the low-level wind deceleration induced by the terrain (Blumen et al., 2001; Newsom and Banta, 2003). As later shown in Figs. 8b and 10b, the terrain slows down the upstream wind at King Plains, enhancing the wind shear. This increased wind shear can destabilize the flow and trigger KHIs. Conversely, once formed, KHIs can feed back on the mean flow by reducing the wind shear and stratification, potentially impacting the spatial variability in wind speed (Section 4.1).."

#GC3 There are several interesting aspects in the discussion section. However, I think some parts of the Discussion section (e.g., Sections 4.2) tend to summarize previous studies in a way that resembles a literature review to me. While providing context is valuable, the main focus should be on interpreting the study's findings in a more quantitative way if it fits and highlighting their contribution to new knowledge. For example, in Sec. 4.2, the paras related to control, TI, and TKE, the authors could provide a more in-depth analysis of their own results, discussing their implications and significance in more detail and quantitative way. Strengthening this aspect would improve the clarity of the study's contributions in order to remain centered on the novel aspects of the research.

We appreciated the reviewer's feedback on the paragraph that discusses the implications of our studies for wind farm control. We have trimmed down some references in that paragraph to make it more focused, and included quantitative metrics to discuss the spatial variability in wind speed, thrust, and wakes. We think that conveys the intended rationale that even sites with simple terrain, under certain atmospheric conditions such as LLJs, can be intricate to implement wind farm control and to represent with numerical models. Thus, challenges associated with spatial gradients in wind are not exclusive to complex terrain sites. The changes are marked in lines 537–560.

"The terrain-induced spatial variability in wind speed acting over different turbines is between 6.7 and 10.7 m s−1 and causes a variability in the region of operation of individual turbine power curves (Fig. C1a,b). As a result, turbines H02–H03 534 experience a smaller thrust force (275 and 308 kN, respectively) than the other turbines (between 362 and 380 kN) (Fig. C1a).."

#GC4 Given the quality of the work and its good coverage of important factors, like including operational aspects such as control and aerodynamic load (e.g., in terms of Ct), I suggest that the authors explicitly discuss the effect of positive and negative shear on aerodynamic load. A brief elaboration in the main text or a relevant citation would enhance the clarity and completeness of the discussion. Additionally, I have come across a couple of reports and publications in recent years that explore multiscale interactions from mesoscale to microscale, down to structural responses, that can be cited for this purpose.

The influence of positive and negative shear on turbine loads is particularly relevant in LLJ conditions due to their strong shear. Gadde et al. (2021) observed that positive shear across the rotor generally enhances axial aerodynamic loads. In strong LLJs, the high nose height ensures that positive shear acts over the entire rotor despite terrain-induced vertical displacements. In contrast, for weaker, shallower LLJs (nose height ~100 m AGL), terrain-induced displacements (~30 m, Figure 12b) may lead to either positive or negative shear across most of the rotor, depending on turbine location.

Atmospheric stability modulates aerodynamic loads, enhancing them via increased wind shear but reducing them through turbulence suppression (Sathe et al., 2013; Porté-Agel, 2020). Strong LLJs could be particularly impactful as they may also generate stronger turbulence compared to weak LLJs and other stable boundary layer conditions.

As the reviewer highlights, this discussion is critical for numerical frameworks coupling atmospheric turbulence to turbine response and loads (Gadde et al., 2021; Trigaux et al., 2024; Grinderslev et al., 2021; Shaler et al., 2024; Kapoor et al., 2020). Notably, Shaler et al. (2024) emphasize the role of spatial variability in inflow on turbine load predictions.

Thus, we have incorporated the following discussion marked in lines 493–497:

"Accounting for the spatial variability of LLJs of different depths is also relevant for turbine loads. Atmospheric stability influences turbine loads by modulating shear and turbulence (Sathe et al., 2013; Porté-Agel, 2020). Strong, high-nose LLJs (Krishnamurty et al., 2025; Figure 6) can increase axial loads due to enhanced shear (Gadde et al., 2021), while weaker, shallower LLJs may expose turbines to negative shear and reduce loads. Neglecting the spatial variability in wind speed can also bias load predictions in multiscale simulations (Shaler et al., 2024)."

Specific comments

#SC1 In line 198-200, authors mention using the Eckert number (Ec) in the calculation of potential temperature perturbation amplitude, based on Muñoz-Esparza and Kosovic (2018), with a value of 0.2. It would be helpful if the authors could include and explain why the Eckert number is important in this context and how it influences the simulation, particularly in relation to the vertical confinement of perturbations and the diagnosed PBL height in this paper. Whether the 0.2 limit for the Eckert number remains the same across different applications, particularly in scenarios involving terrain effects. Does the presence of terrain influence the chosen value for the Eckert number, or is it considered a constant in all cases?

As discussed in Muñoz-Esparza and Kosović (2018), the Ec of 0.2 proves to be adequate for stably-stratified conditions with perturbations applied within the diagnosed boundary-layer height (which was here about 500 m AGL). Further, Muñoz-Esparza et al. (2017) apply the cell perturbation method in terrain of similar complexity as studied here (the CWEX domain) and also find Ec of 0.2 to be adequate. Lastly, Connolly et al. (2020) used the cell perturbation method in the highly complex terrain of the Perdigão field campaign in Portugal with an Ec of 0.2. They found that the perturbations improved the representation of turbulence compared to the turbulence generated from the complex terrain itself.

We have incorporated these references in the manuscript to substantiate our choice of Ec = 0.2 in lines 212–214, as explicitly mentioned that the perturbations are constrained to the PBLH of about 500 m AGL (marked line 211):

"The potential temperature perturbation amplitude was calculated based on Muñoz-Esparza and Kosović (2018) for a turbulent Eckert number (Ec) of 0.2, which was effective in several applications in simple (Muñoz-Esparza and Kosović, 2018; Sanchez Gomez et al., 2022) and complex terrain (Connolly et al. ,2020)."

#SC2 How does your model avoid feedback between the turbulent signal in the buffer zone and the inflow boundary for the terrain simulation? More specifically, in your simulations with realistic land surface distributions, as well as simple terrain, does the method rely on statistically homogeneous turbulence within the buffer zone? If so, how can it be ensured that statistically homogeneous turbulence is achievable when large buffer zones are added?

We thank the reviewer for this insightful question. In our setup, there is no feedback between the buffer zone and the inflow boundary because the nested domains are one-way coupled. Furthermore, the CPM does not rely on statistically homogeneous turbulence in the buffer zone. The goal is not to impose homogeneity, but rather to accelerate the development of realistic turbulence given the mesoscale inflow conditions, which are applied as Dirichlet boundary conditions in WRF.

While the CPM was originally tested under idealized conditions with horizontally homogeneous flow and statistically homogeneous turbulence, its intended and proven application is in realistic multiscale simulations. In such settings, topographic and land surface heterogeneity naturally lead to spatially variable turbulence and mean flow structures. The method has been successfully applied in several studies over both simple (Muñoz-Esparza et al., 2017; Arthur et al., 2020; Sanchez Gomez et al., 2022; this study) and complex terrain (Connolly et al., 2020; Wise et al., 2022), demonstrating its suitability for cases where statistical homogeneity cannot be assumed.

#SC3 Aligned with above, for the innermost domain, to shorten the fetch required for turbulent spin-up (lines 196-198), cell perturbation has been used. However, the effects of this method are not limited to the potential temperature or velocity fields; it may also induce unrealistic thermodynamic conditions. This highlights the importance of having sufficient buffer zones at the inflow boundaries, where turbulence can develop spatially. As noted by Mirocha et al. (2014), who showed that without perturbations, a fetch length of several tens of kilometers is needed to achieve fully developed turbulence, meaning that a significant portion of computational resources is spent on these buffer zones. You mention in lines 202-203 that spinning up occurs between 1.5 and 2 km from the southerly boundary of D3.

However, I believe more detail is needed on the turbulence recycling process, particularly how it contributes to computational efficiency and results in faster spin-up.

As the reviewer points out, the value of the CPM is in avoiding wasting extensive fetch in buffer zones. The CPM can reduce the required upstream fetch by a factor of 4–5 (Muñoz-Esparza and Kosović, 2018). Extrapolating that information to our case, we would need an upstream fetch of about 6–10 km to have fully developed turbulence, which could triple the computational cost.

We would like to clarify that turbulence recycling is not in fact used in these simulations. Similar to our previous response to the reviewer, there is no feedback between the buffer zone and the inflow boundary because the nested domains are one-way coupled.

Thus, we have mentioned the computational benefits of the CPM marked in lines 218–219:

"Without the CPM, upstream fetches 4–5 times longer would be needed (Muñoz-Esparza and Kosović, 2018), doubling domain size and computational cost."

#SC4 Given that the Kelvin-Helmholtz Instabilities (KHIs) are observed near the third row and below the LLJ nose, and are not caused by the turbines (as they also occur in the simulation without turbines), could the authors elaborate on the specific factors contributing to the formation of KHIs in this region (e.g. small Richardson number, …)? Are these instabilities primarily driven by shear in the wind profiles? You may slightly elaborate here with citation of any related reference on this process, for the region.

The KHI is generally understood as a competition between shear and buoyancy forces, expressed by the Richardson number (Stull, 1988). Strong stratification suppresses vertical motion but also leads to flow decoupling, which increases shear. The increased shear can destabilize the flow (dynamic instability) and overcome buoyancy suppression, ultimately creating a KHI.

The commonly reported mechanism for KHI generation is enhanced wind shear in stable boundary layers (SBLs) (Newsom and Banta, 2003; Blumen et al., 2001). For instance, Newsom and Banta (2003) describe how low-level wind deceleration enhances wind shear, leading to KHIs. Cold air pooling from drainage flows can also create stagnant near-surface winds capped by a strong potential temperature gradient, which induces shear-driven instabilities (Zhou and Chow, 2014).

In a prior NAWEA presentation, Wise et al. (2022) examined the sensitivity of KHI formation to the specific shear (S) and buoyancy (N) values used in the Richardson number calculation, where $Ri = N^2/S^2$. He observed that KHI typically developed when $Ri \approx 0.25$, as expected, but the result was highly sensitive to the height range used for

gradient calculations. Moreover, while both increased shear and reduced buoyancy can trigger instability, distinguishing their relative contributions is challenging. Again, the increased shear and turbulent mixing could be the underlying cause for the reduction in stratification.**

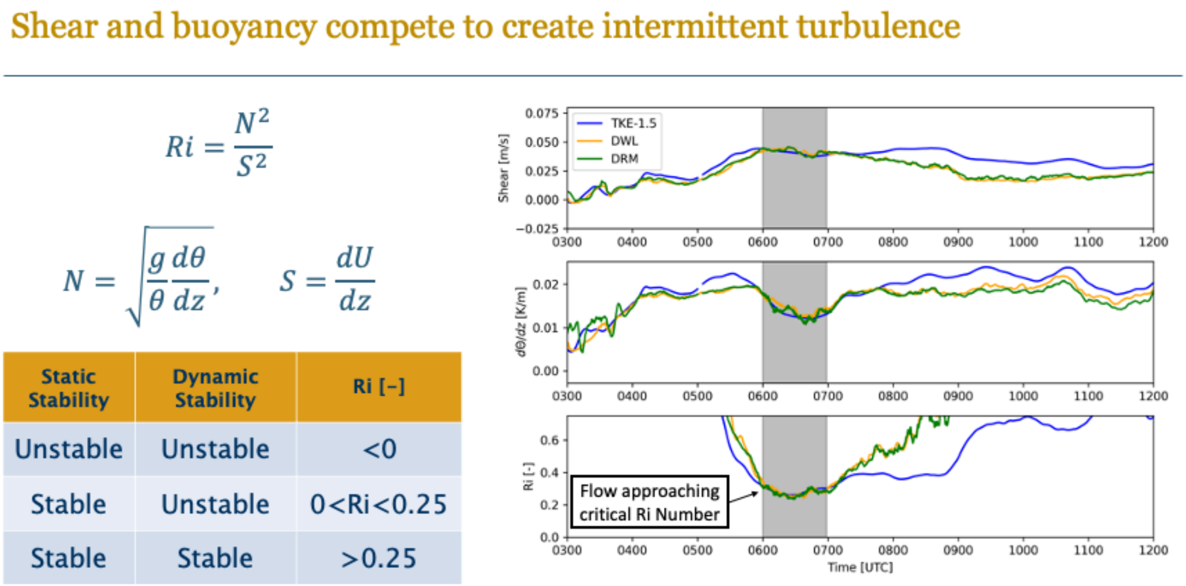

Figure – Slide of a NAWEA presentation by Wise et al. (2022).

We have expanded our discussion of KHI formation with additional references (line 308), tying our findings to established mechanisms in the literature, marked in lines 318–322:

"A plausible explanation for the observed KHI formation in our investigation is the low-level wind deceleration induced by 316 the terrain (Blumen et al., 2001; Newsom and Banta, 2003). As later shown in Figs. 8b and 10b, the terrain slows down the upstream wind at King Plains, enhancing the wind shear. This increased wind shear can destabilize the flow and trigger KHIs. Conversely, once formed, KHIs can feed back on the mean flow by reducing the wind shear and stratification, potentially impacting the spatial variability in wind speed (Section 4.1)."

#SC5 In Figure 7 and Section 3.4, I am curious about the presence of Kelvin-Helmholtz instability (KHI) in Figures 7b and 7d and whether such instability (dynamical instability) could potentially influence streamline vertical displacement or have any potential impact on the overall flow field.

We have addressed this comment made by the reviewer in the General comment #2, where we stated that "the KHIs can influence the spatial variability in wind speed by enhancing vertical momentum transport and weakening thermal stratification. Specifically, the enhanced mixing (i) can transport momentum downward from the LLJ core, accelerating wake recovery, while the altered mean state (ii) can increase

near-surface wind speeds and reduce stratification. These changes act to reduce the terrain-induced spatial heterogeneity in wind speeds, as discussed in Section 4.1.”

Additionally, we briefly discuss this in the new paragraph on lines 315–318 to acknowledge the role of KHIs without diverting too much from our primary focus.

“A plausible explanation for the observed KHI formation in our investigation is the low-level wind deceleration induced by 316 the terrain (Blumen et al., 2001; Newsom and Banta, 2003). As later shown in Figs. 8b and 10b, the terrain slows down the upstream wind at King Plains, enhancing the wind shear. This increased wind shear can destabilize the flow and trigger KHIs. Conversely, once formed, KHIs can feed back on the mean flow by reducing the wind shear and stratification, potentially impacting the spatial variability in wind speed (Section 4.1).”

#SC6 In lines 327–336, a clearer and more quantitative explanation would be beneficial. The discussion relies on Figures C1a and C1b to explain thrust coefficient behavior, but it is somewhat unclear whether these figures present direct empirical data, simulation results, or theoretical curves. Could you clarify this? Additionally, including specific Ct values or a comparative table would enhance clarity.

The curves in Figures C1a and b are theoretical and as obtained in the OpenFAST implementation based on the scaling of an IEA turbine to emulate the GE 2.8 MW turbines installed in King Plains, whose detailed specifications are proprietary. The turbine rotor speed and pitch curves vs. inflow wind speed and the blade aerodynamic properties that produce those curves are used in the GAD. We improved this description in the Appendix C, marked in lines 656–662:

“The theoretical curves shown in Fig. C1a,b are derived from the OpenFAST implementation, where an IEA reference turbine was scaled to approximate the characteristics of the GE 2.8 MW turbines installed in King Plains (Quon, 2022). Since the detailed specifications of these turbines are proprietary, this scaling provides a representative but not exact model. The GAD approach does not directly use these curves. Instead, it relies on the same turbine rotor speed and pitch control curves, along with the blade aerodynamic properties, that generate the power and thrust curves in OpenFAST. The GAD then computes the axial and tangential forces acting on the rotor disks, which in turn influence the momentum tendencies (Mirocha et al., 2014; Aitken et al., 2014; Arthur et al., 2020).”

We have also improved the discussion with more quantitative metrics based on Figure C1a and b, explicating individual turbine inflow wind speeds and expected thrust forces, marked in lines 357–367:

“This variability can be explained by the slower inflow wind speeds for H02 (6.7 m s−1) and H03 (7.1 m s−1) in comparison with the remaining turbines (7.7–10.7 m s−1), which at these wind speeds, considering the thrust coefficient variability of this turbine, produce a smaller thrust force (275 and 308 kN, respectively) and thus a weaker wake (Fig. C1a). The expected thrust of the remaining turbines is between 362 and 380 kN and hence closer to the maximum value of 380 kN in the thrust curve. Another possible explanation for the shorter wake of H02–H03 could be the relatively stronger wake-added turbulence caused by the higher Ct that can enhance wake recovery (Letizia and Iungo, 2022). Even if the thrust is lower in an absolute sense, H02–H03 (Ct ~0.79) are expected to have a higher coefficient of thrust (Ct) compared to the other generators in the domain (Ct between 0.42 and 0.79) and based on the Ct vs WS curve (Fig. C1b).”

Even though the thrust force and loads discussion is relevant, more focused future work with the explicit evaluation of thrust forces would be better equipped to explore these relations. Furthermore, the role of the streamwise pressure gradient forces induced by the terrain on wake recovery should also be explored (Porté-Agel, 2020). We thus keep our focus on the spatial variability in wind speed and turbine power relations.

#SC7 Since you are using an ADM, I assume you may have access to along-the-blade thrust force distributions or at least the total thrust force from the model. I suggest more quantitative details on this and refine the explanation accordingly.

We appreciate the reviewer's insightful suggestion regarding the thrust force distributions obtained from the Generalized Actuator Disk (GAD) model. While the GAD model does compute thrust forces at the rotor disk, these variables were not configured to be output in our current simulations, as our primary focus was on the spatial variability of winds and power performance. Consequently, we do not have access to detailed aerodynamic load data from these runs. We acknowledge the value of such quantitative details and will consider incorporating them in future studies to enhance our analysis.

#SC8 In Figure 9, analyzing turbulence intensity, alongside the given shear and veer studies by authors, can provide a better understanding of how terrain influences wake behavior in the wind park, as well as the relationship between TI and wake characteristics and recovery. I recommend authors could comment and elaborate on this.

We appreciate the reviewer's insightful comments regarding the analysis of turbulence intensity (TI) in relation to shear, veer, and wake behavior within the wind park. In response, we have evaluated time-averaged hub-height variables such as turbulent kinetic energy (TKE), TI, vertical wind velocity, and the standard deviation of the x-component of wind velocity (a proxy for wind direction variability). Our analysis reveals spatial variability in these variables; however, the variations are not substantial. Notably, the values for TKE and TI near turbines H02 and H03 do not indicate factors

that would contribute to faster wake recovery in that region. Additionally, vertical wind velocity is not significantly elevated, suggesting that vertical displacement of wakes is not a contributing factor.

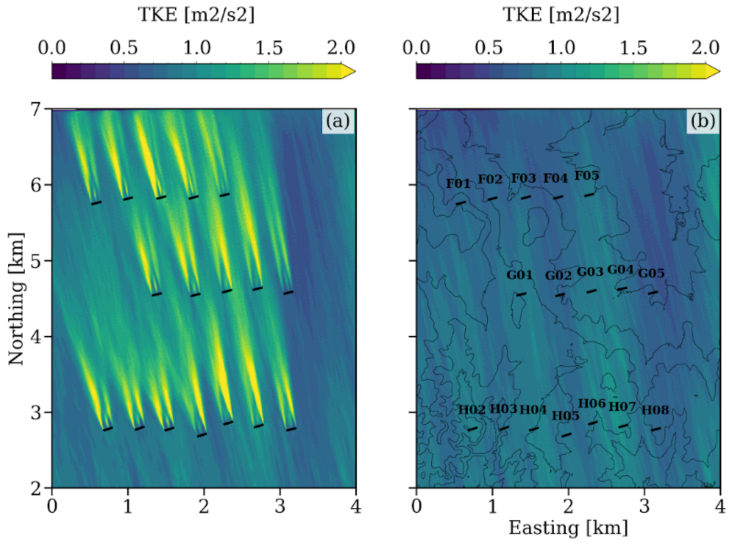

Figure – Time averaged TKE at hub height for the simulation with (a) and without (b) turbines.

The most plausible hypothesis for the faster wake recovery for turbines H02 and H03 is their lower thrust force (Figure C1a). Based on the average wind speed at each turbine, we observe that the thrust force (green curve) associated with wind speeds near 7 m/s is significantly smaller than at the other turbines. Thus, the spatial variability in wind speed leads to a reduced thrust force in turbines H02 and H03, and consequently, a shorter wake.

An improved account for the spatial variability of the wakes is briefly provided, marked between lines 357–367:

"This variability can be explained by the slower inflow wind speeds for H02 (6.7 m s−1) and H03 (7.1 m s−1) in comparison with the remaining turbines (7.7–10.7 m s−1), which at these wind speeds, considering the thrust coefficient variability of this turbine, produce a smaller thrust force (275 and 308 kN, respectively) and thus a weaker wake (Fig. C1a). The expected thrust of the remaining turbines is between 362 and 380 kN and hence closer to the maximum value of 380 kN in the thrust curve. Another possible explanation for the shorter wake of H02–H03 could be the relatively stronger wake-added turbulence caused by the higher Ct that can enhance wake recovery (Letizia and Iungo, 2022). "

Technical corrections and minor comments

#MC1 In the caption of Fig. 2, it appears that the domains are related to WRF, but clarifying whether they are mesoscale or microscale would be helpful. For example, the inner domain, as mentioned in lines 152 and 162, corresponds to the LES domain.

We have improved the caption in Figure 2 to explicitly refer to domain D1 as a mesoscale domain, and domains D2 and D2 as LES domains.

"Figure 2. Horizontal extent and terrain elevation maps associated with the WRF simulations mesoscale domain D1 (a) and LES domains D2 (b) and D3 (c). The King Plains wind farm consists of 88 turbines (white dots), from which a subset of 17 wind turbines was represented in the simulation (black dots). Within domain D3, some turbines near boundaries were removed (white dots). Inflow fetches of 2 and 1~km in the southerly and easterly boundaries, respectively, were removed from the analyses (white dashed lines). The observation sites A1, A2 and C1 (black triangles) are also shown."

#MC2 In lines 172-173, the authors use the term 'simulations forced...'. While it is somewhat clear that the forcing files are from ERA5, the word 'forced' may give the impression of data assimilation, at least for me. While this is not necessarily incorrect, it would be helpful if the authors could slightly modify here to avoid potential confusion.

We have changed the term 'forced' to 'driven', and linked the driven to initial and boundary conditions so as not to mislead the reader toward data assimilation.

"In this case study, simulations driven by initial and boundary conditions from the European Centre for Medium-Range Weather Forecasts Reanalysis v5 (ERA5).."

#MC3 Minor comment: The paper discusses the effect of terrain on wind speed but does not specify properly the extent of lateral inhomogeneity required to observe significant changes. A quantitative measure of inhomogeneity (e.g., spatial correlation metrics) in the wind field during the study events would help clarify this aspect. This is particularly important given the discussion on terrain-induced accelerations, "even with simple topographic features, potentially causing substantial changes in wind speed and wind farm performance" (see lines 74–75). Additionally, it directly relates to the first study objective outlined in lines 86–87.

The Figure below shows that there is important lateral variability in the lateral direction, especially near the first row of turbines (Northing ~ 3 km). The difference between the minimum and maximum wind speed at Northing = 2.37 and 3.14 km is 2.82 and 2.52 m/s, respectively. This difference in wind speed is responsible for the variability in power performance within the same row of turbines (Figure C1a). The

difference in wind speed is largest in the streamwise direction, though. The difference between the minimum and maximum wind speed at Easting = 0.49 and 1.05 km is 4.12 and 4.22 m/s, respectively. As for the lateral variability in the streamwise gradients in wind speed, it varies from a minimum of 1.85 m/s at Easting = 3.83 km to a maximum of 4.22 m/s at 1.05 km. An average value for the whole domain would be 3.06 m/s, which confirms a sustained pattern of streamwise gradients. We opted not to include these additional results, as Figs. 8b and provide a reasonable illustration that the streamwise gradients in wind speed are generally sustained across the domain, and are not merely episodic in the north-south transects represented in Figs. 10, 11 and 12.

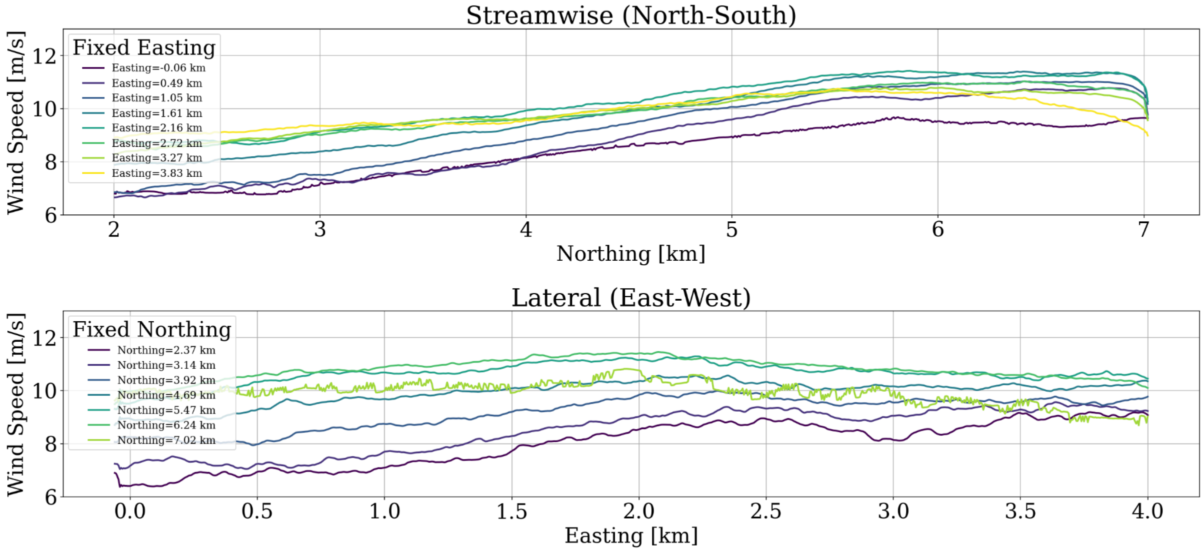

Figure – Time-averaged wind speed at hub height for domain D3 in the simulation without turbines probed at equally-spaced intervals in the streamwise and lateral directions.

#MC4 Minor comment: While selecting a stationary window—where wind speed and large-scale forcing remain relatively steady—might be reasonable, could you clarify which dynamic events are relevant to this region? For example, are you referring to large-scale weather systems such as cold fronts, synoptic-scale cyclones, or other mesoscale influences? Lines 127-128.

The stationary window is chosen to exclude larger-scale and synoptic processes, such as cold fronts and cyclones, as the reviewer correctly notes. Additionally, mesoscale processes with longer timescales, such as drainage flows from mountains or sloping terrain extending over hundreds of kilometers, are undesirable, as they introduce significant temporal variations in mean wind speed, direction, and stratification. However, submeso motions, including drainage flows associated with smaller-scale topographic features, are an inherent part of stable boundary layer (SBL) dynamics (Mahrt, 2009) and are therefore considered in the analysis. Thus, we have included the following statements in the revised text:

“The stationary window excludes larger-scale processes like cold fronts and cyclones, as well as mesoscale drainage flows over hundreds of kilometers, which cause significant wind and stratification changes. However, submeso motions, including drainage flows from smaller topographic features, are inherent to stable boundary layer dynamics (Mahrt, 2009) and are included in the analysis.”

#MC5 I may have overlooked something in Section 3.3—could you clarify what resolution is required to realistically simulate KH waves in WRF? (whether In all domains, WRF is able to resolve it ?, I assume no)? Additionally, since potential temperature serves as a useful metric for identifying wave overturning, I’m curious about how KHI responds to the selection of microphysics schemes. While this might extend beyond the immediate scope of your study, it would still be valuable if you could reference any relevant studies on KH waves in this context and area.

The required resolution depends on the length scale associated with the KHI episode at that particular location. Although the KHI has a multiscale cascade of eddies, we assess the spatial resolution required to resolve the largest instabilities. Judging by our Figure 7, the largest instabilities have a length scale in the range between 100 and 200 m. Thus, it would most likely be resolved by grids finer than 15–30 m, considering the grid's effective resolution as the grid resolution times 7 (DX*7) (Skamarock, 2004). Thus, the KHI would only be resolvable by the innermost domain D3 (DX = 5 m). In Zhou and Chow (2014), they successfully simulated a shear instability with a grid resolution of 25 m for the 1999 Cooperative Atmosphere-Surface Exchange Study (CASES-99) site in Kansas. They reported that the instability was unresolved with a grid resolution of 128 m. In Conrick et al. (2018), KHIs of much larger spatial scales (3–5 km) were investigated, and they similarly report that only the finest domain with a grid resolution of 444 m was able to resolve it.

The relationship between the KHI and microphysical variables was investigated in detail by Conrick et al. (2018). With multiscale WRF simulations with nested domains with grid resolutions from 36 km to 444 m, they evaluated 3 microphysics schemes: Morrison double-moment scheme2 (MORR2), Thompson, and WSM63. The amplitude of vertical motion is reduced with Morrison and WSM6 in comparison with the Thomson scheme, which is associated with the formation of graupel hydrometeor loading, which reduces updraft speeds.

We have incorporated a paragraph with a new citation to Conrick et al. (2018), including other references, to improve the links between KHI and modeling choices, such as grid resolution and microphysics schemes:

“The largest instabilities have length scales ranging from 100 to 200 m. Given that the effective resolution of a numerical model is approximately seven times the grid spacing (7DX) (Skamarock, 2004), resolving these instabilities requires a grid finer than 15--30

m. Therefore, the KHI is only resolvable in the innermost domain, D3 ($\Delta x=$~5~m). This constraint is consistent with findings in the KHI literature (Zhou and Chow, 2014; Conrick et al., 2018). Additionally, the influence of microphysics schemes on KHI is examined in detail by Conrick et al. (2018).”

#MC6 Minor comment: Furthermore, is there a way to improve the representation of Figure C1? Perhaps an alternative visualization or additional annotations?.

We incorporated an annotation (“increasing turbine inflow wind speed”) and a right-pointing arrow in Figure C1 that better indicates the meaning of the colored vertical lines associated with turbine inflow wind speeds. The Figure conveys the turbine theoretical curves and locates the individual turbines in those curves, which supports the discussions on the spatial variability in power performance and wakes.

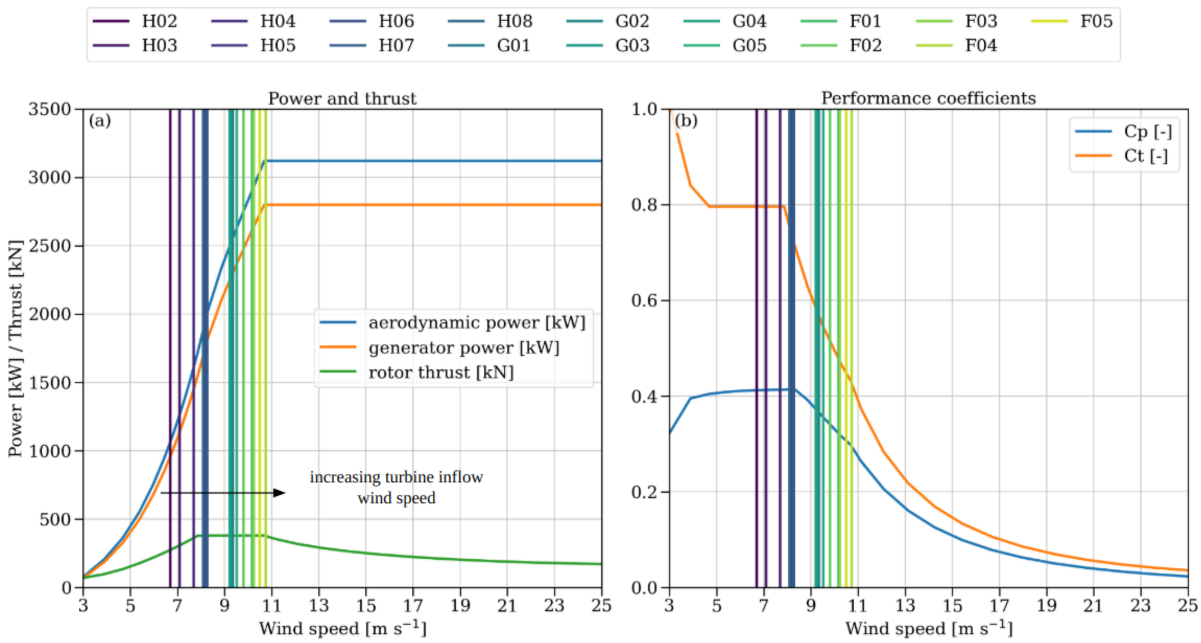

#MC7 Minor comment: In lines 345-346 for the sake of more clarity, do you mean something like? : The initial terrain-induced up- and downward motions trigger disturbances, and the buoyancy restoring forces sustain the resulting undulations in the flow.

We appreciate the reviewer's insightful suggestion regarding lines 345–346. In response, we have revised the sentence to:

“The buoyancy restoring forces acting on the initial, terrain-triggered up- and downward motions create and sustain the undulations.”

This adjustment aims to enhance clarity and accurately convey the intended meaning.

References

Arthur, R. S., Mirocha, J. D., Marjanovic, N., Hirth, B. D., Schroeder, J. L., Wharton, S., & Chow, F. K. (2020). Multi-scale simulation of wind farm performance during a frontal passage. *Atmosphere, 11*(3), 1–17. https://doi.org/10.3390/atmos11030245

Banta, R. M., Newsom, R. K., Lundquist, J. K., Pichugina, Y. L., Coulter, R. L., & Mahrt, L. (2002). Nocturnal low-level jet characteristics over Kansas during CASES-99. *Boundary-Layer Meteorology, 105*(2), 221–252. https://doi.org/10.1023/A:1019992330866

Blumen, W., Banta, R., Burns, S. P., Fritts, D. C., Newsom, R., Poulos, G. S., & Sun, J. (2001). Turbulence statistics of a Kelvin-Helmholtz billow event observed in the night-time boundary layer during the Cooperative Atmosphere-Surface Exchange Study field program. *Dynamics of Atmospheres and Oceans, 34*(2–4), 189–204. https://doi.org/10.1016/S0377-0265(01)00067-7

Connolly, A., van Veen, L., Neher, J., Geurts, B. J., Mirocha, J., & Chow, F. K. (2020). Efficacy of the Cell Perturbation Method in Large-Eddy Simulations of Boundary Layer Flow over Complex Terrain. *Atmosphere, 12*(1), 55. https://doi.org/10.3390/atmos12010055

Conrick, R., Mass, C. F., & Zhong, Q. (2018). Simulated Kelvin-Helmholtz waves over terrain and their microphysical implications. *Journal of the Atmospheric Sciences, 75*(8), 2787–2800. https://doi.org/10.1175/JAS-D-18-0073.1

Coulter, R. L., & Doran, J. C. (2002). Spatial and temporal occurrences of intermittent turbulence during CASES-99. *Boundary-Layer Meteorology, 105*(2), 329–349. https://doi.org/10.1023/A:1019993703820

Gadde, S. N., Liu, L., & Stevens, R. J. A. M. (2021). Effect of low-level jet on turbine aerodynamic blade loading using large-eddy simulations. *Journal of Physics: Conference Series, 1934*(1). https://doi.org/10.1088/1742-6596/1934/1/012001

Grinderslev, C., Sørensen, N. N., Horcas, S. G., Troldborg, N., & Zahle, F. (2021). Wind turbines in atmospheric flow: Fluid-structure interaction simulations with hybrid turbulence modeling. *Wind Energy Science, 6*(3), 627–643. https://doi.org/10.5194/wes-6-627-2021

Kapoor, A., Ouakka, S., Arwade, S. R., Lundquist, J. K., Lackner, M. A., Myers, A. T., Worsnop, R. P., & Bryan, G. H. (2020). Hurricane eyewall winds and structural

response of wind turbines. *Wind Energy Science, 5*(1), 89–104. https://doi.org/10.5194/wes-5-89-2020

Kasper, J. H., Stieren, A., & Stevens, R. J. A. M. (2024). Simulation and modeling of wind farms in baroclinic atmospheric boundary layers. *Journal of Renewable and Sustainable Energy, 16*(6), 1–15. https://doi.org/10.1063/5.0220322

Krishnamurthy, R., Newsom, R. K., Kaul, C. M., Letizia, S., Pekour, M., Hamilton, N., Chand, D., Flynn, D., Bodini, N., & Moriarty, P. (2025). Observations of wind farm wake recovery at an operating wind farm. *Wind Energy Science, 10*(2), 361–380. https://doi.org/10.5194/wes-10-361-2025

Mahrt, L. (2009). Characteristics of submeso winds in the stable boundary layer. *Boundary-Layer Meteorology, 130*(1), 1–14. https://doi.org/10.1007/s10546-008-9336-4

Malekmohammadi, S., Cheynet, E., & Reuder, J. (2025). Observation of Kelvin–Helmholtz billows in the marine atmospheric boundary layer by a ship-borne Doppler wind lidar. *Scientific Reports, 15*(1), 1–14. https://doi.org/10.1038/s41598-025-89554-4

Muñoz‐Esparza, D., Lundquist, J. K., Sauer, J. A., Kosović, B., & Linn, R. R. (2017). Coupled mesoscale-LES modeling of a diurnal cycle during the CWEX-13 field campaign: From weather to boundary-layer eddies. *Journal of Advances in Modeling Earth Systems, 9*(3), 1572–1594. https://doi.org/10.1002/2017MS000960

Newsom, R. K., & Banta, R. M. (2003). Shear-flow instability in the stable nocturnal boundary layer as observed by Doppler lidar during CASES-99. *Journal of the Atmospheric Sciences, 60*(1), 16–33. https://doi.org/10.1175/1520-0469(2003)060<0016:SFIITS>2.0.CO;2

Porté-Agel, F., Bastankhah, M., & Shamsoddin, S. (2020). Wind-Turbine and Wind-Farm Flows: A Review. *Boundary-Layer Meteorology, 174*(1), 1–59. https://doi.org/10.1007/s10546-019-00473-0

Sanchez Gomez, M., Lundquist, J. K., Mirocha, J. D., Arthur, R. S., Muñoz-Esparza, D., & Robey, R. (2022). Can lidars assess wind plant blockage in simple terrain? A WRF-LES study. *Journal of Renewable and Sustainable Energy, 14*(6), 063303. https://doi.org/10.1063/5.0103668

Sathe, A., Mann, J., Barlas, T., Bierbooms, W. A. A. M., & van Bussel, G. J. W. (2013). Influence of atmospheric stability on wind turbine loads. *Wind Energy*, *16*(7), 1013–1032. https://doi.org/10.1002/we.1528

Shaler, K., Quon, E., Ivanov, H., & Jonkman, J. (2024). Wind farm structural response and wake dynamics for an evolving stable boundary layer: computational and experimental comparisons. *Wind Energy Science*, *9*(7), 1451–1463. https://doi.org/10.5194/wes-9-1451-2024

Skamarock, W. C. (2004). Evaluating mesoscale NWP models using kinetic energy spectra. *Monthly Weather Review*, *132*(12), 3019–3032. https://doi.org/10.1175/MWR2830.1

Smith, E. N., Gebauer, J. G., Klein, P. M., Fedorovich, E., & Gibbs, J. A. (2019). The great plains low-level jet during PECAN: Observed and simulated characteristics. *Monthly Weather Review*, *147*(6), 1845–1869. https://doi.org/10.1175/MWR-D-18-0293.1

Zhou, B., & Chow, F. K. (2012). Turbulence modeling for the stable atmospheric boundary layer and implications for wind energy. *Flow, Turbulence and Combustion*, *88*(1–2), 255–277. https://doi.org/10.1007/s10494-011-9359-7

Zhou, B., & Chow, F. K. (2014). Nested large-eddy simulations of the intermittently turbulent stable atmospheric boundary layer over real terrain. *Journal of the Atmospheric Sciences*, *71*(3), 1021–1039. https://doi.org/10.1175/JAS-D-13-0168.1

Wise, A. S., Neher, J. M. T., Arthur, R. S., Mirocha, J. D., Lundquist, J. K., & Chow, F. K. (2022). Meso- to microscale modeling of atmospheric stability effects on wind turbine wake behavior in complex terrain. *Wind Energy Science*, *7*(1), 367–386. https://doi.org/10.5194/wes-7-367-2022

Wise, A.S., Arthur, R.S., Mirocha, J.D., Lundquist, J.K., Chow, F.K. Wind turbine performance under a range of stable boundary layer conditions. NAWEA/WindTech Conference, Newark, DE, 2022.